Structural Eng./Earthquake Eng., JSCE, Vol. 19, No. 2 [Special Issue], 179s—197s, 2002 October

DAMAGE OF BRIDGES RESULTING FROM FAULT RUPTURE IN THE 1999 KOCAELI AND DUZCE, TURKEY EARTHQUAKES AND THE 1999 CHI-CHI, TAIWAN EARTHQUAKE

Kazuhiko KAWASHIMA[1]

[1]Professor, Department of Civil Engineering, Tokyo Institute of Technology
(O-Okayama, Meguro, Tokyo 152-8552, Japan)

This paper describes the damage of bridges resulting from the fault movements in the 1999 Kocaeli and Duzce, Turkey, Earthquakes and the 1999 Chi-Chi, Taiwan, Earthquake. Effect of the fault displacement on the seismic performance of bridges is presented with an emphasis on the mechanism of failure.

Key Words : *seismic damage, bridge, fault rupture, Turkey, Kocaeli Earthquake, Duzce Earthquake, Taiwan, Chi-Chi Earthquake*

1. INTRODUCTION

In the Kocaeli Earthquakes (moment magnitude M_w=7.4), August 19, 1999 and the Duzce Earthquake (moment magnitude M_w=7.2), November 12, 1999 in Turkey, and the Chi-Chi Earthquake (M_w=7.6), September 21, 1999 in Taiwan, it was apparent that in addition to the near-field ground motion effects, the fault displacement was a major threat to the transportation facilities. Since the possibility that a bridge directly suffers damage resulting from a tectonic fault displacement has been limited in the past earthquakes, measures for the fault rupture have been disregarded in seismic design of bridges. However, the above three earthquakes revealed the fact that appropriate measures are required for the fault ruptures at the locations where a bridge crosses a causative fault.

Since the damage of structures directly resulted from fault ruptures has been quite few, it is important to collect information on the damage mechanism. This paper presents the damage of bridges that was resulted from the fault rupture in the Kocaeli, Duzce and Chi Chi Earthquakes. Since many documents are available for the damage due to the ground excitation effects, only the damage resulting from the faults is presented here.

2. KOCAELI, TURKEY, EARTHQUAKE

(1) Fault displacements and ground motions in the damaged area

In the Kocaeli earthquake, the transportation facilities suffered extensive damage in the Sakarya region. A part of the right-lateral strike slip Anatolian fault ruptured in east-west direction for about 100km from Golcuk to Duzce. As shown in **Fig. 1**, since the Trans-European Motorway was almost parallel to the fault, the fault crossed the Motorway at several locations. Extensive damage occurred at these intersections. Damage of the road facilities was extensive around the city of Arifiye as shown in **Figs. 2** and **3**. Arifiye Overpass (No. 3, refer to **Fig. 3**) and Sakarya Center Bridge (No. 5, refer to **Fig. 3**) collapsed. Overpasses near Ariyiye Overpass (No. 1, 2, 4 and 5, refer to **Fig. 3**) suffered limited damage. Since Fig. 3 was produced based on

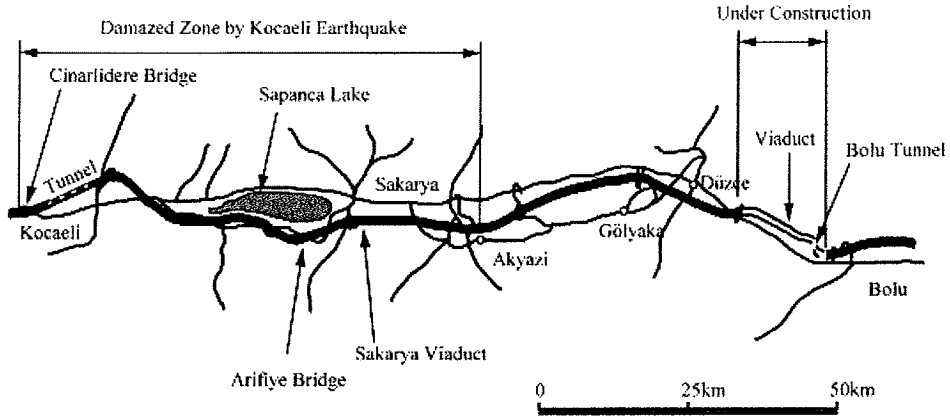

Fig.1 Damaged Region in the Kocaeli and Duzce Earthquakes, Turkey

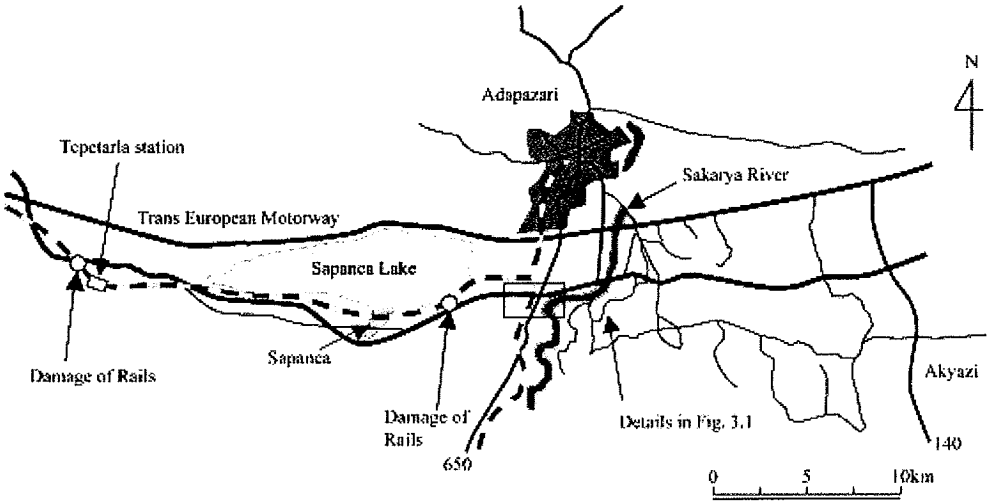

Fig.2 Damaged Area near Sapancia Lake

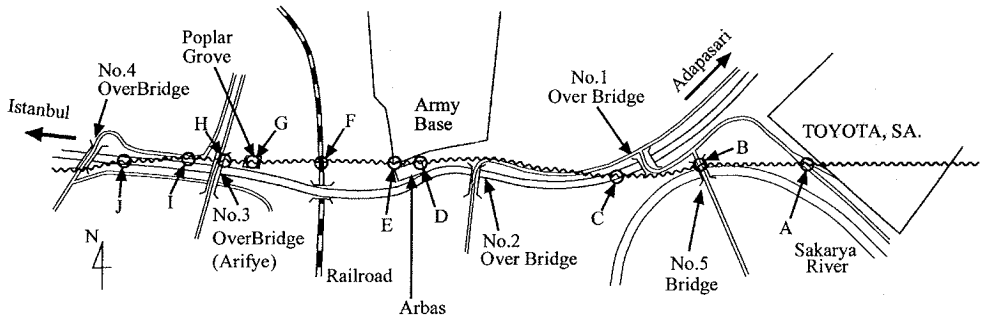

Fig.3 Damaged Transportation Facilities and Fault-Induced Ground Movement, Kocaeli Earthquake

the author's memo during the survey, it may not be geometrically exact.

Various evidences of the right-lateral strike slip rupture were observed in the area (refer to **Fig. 3**) [1), 2), 3)]. A 4.3m offset of a concrete fence occurred at an automobile factory (Arbas Arac Kadlama Fabzikasi) at its northeast corner (Point D) as shown in **Photo 1**. In a poplar grove at Point G, the fault offset measured from the displaced poplar trees was as large as 4.3m, as shown in **Photo 2**. The fault resulted in an offset of a 1m-diameter sewer pipe embedded at Point H, as shown in **Photo 3**. The offset appeared to be in the order of at least 3m and probably 4m. The fault rupture continued further west parallel to the Motorway

Photo 1 4.3m Offset of a Concrete Fence at Automobile Factory (Point D, refer to Fig. 3)

Photo 2 4.3m Offset of Poplar Trees at Point G (Refer to Fig. 3)

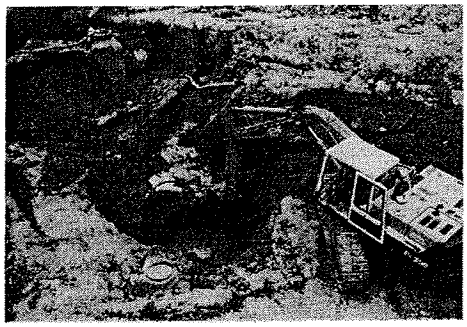

Photo 3 Offset of a Sewage Pipe at Point H (Point D, refer to Fig. 3)

Photo 4 3.6m Offset of a Drainage Pipe at Point H (Refer to Fig. 3)

Photo 5 2.5m Offset of Poplar Trees near Tepetarla Station (South side (bottom in Photo) was about 1m lower than the north side (top))

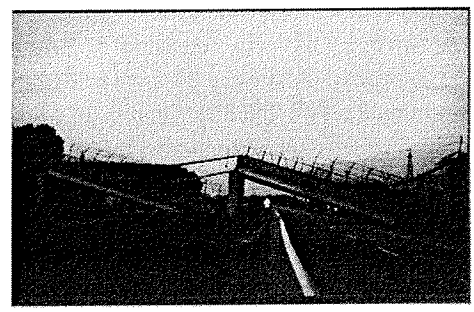

Photo 6 Collapse of Arifiye Bridge H

and resulted in a 3.6m offset of a 1.4m-diameter drainage pipe at Point I, as shown in **Photo 4**. The Points G, H and I were close to Arifiye Bridge that collapsed in the earthquake.

Near Tepetarla Station (refer to **Fig. 2**) where a large offset of railways occurred, an offset of the poplar trees of about 2.5m occurred as shown in **Photo 5**. As well as the right lateral slip, a vertical offset occurred (south tip of the fault was about 1 m lower than the north tip).

Strong ground accelerations were recorded at several locations by the Ministry of Public Works and Settlement, Bogazici University and Istanbul Technical University[4]. **Fig. 4** shows the ground accelerations recorded at Sakarya, Adapazeri. The fault normal acceleration was not recorded at this site. The peak acceleration of the fault parallel component was 4.07m/s^2, and this was the highest acceleration measured in the Kocaeli earthquake. It was rather smaller than the amplitude that is generally generated by an M_w 7.4 earthquake. The response acceleration was over 1g at short natural period, but it decreased sharply as the period increased.

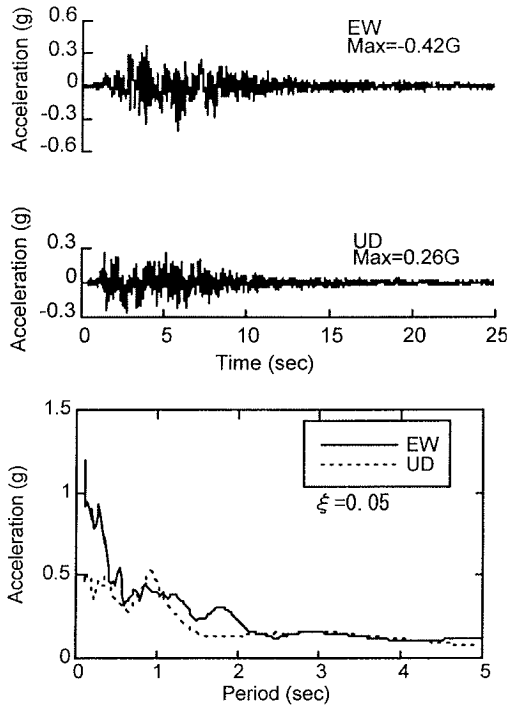

Fig. 4 Ground Motions Recorded at Sakarya, Adapazeri

(2) Collapse of Arifiye Overpass

The Arifiye Overpass consisted of four span simply supported prestressed concrete bridge (No. 3, refer to **Fig. 3**). Two abutments and three wall-type reinforced concrete piers supported the deck. It was a skewed bridge with an angle of 65-degree. The substructures and the decks are denoted herein as A1, P1, P2, P3 and A2, and D1, D2, D3 and D4, respectively, from the north to south (refer to **Fig. 5**). As shown in **Photo 6**, D2, D3 and D4 fell down at their south ends with the north ends still being supported by the piers.

The decks consisted of 5 precast concrete U-beams as shown in **Fig. 6**. Five elastomeric bearings with a size of 300mm x 300mm and 100mm high supported the deck per substructure. As shown in **Fig. 7**, the piers were 1m thick and 14m wide in the longitudinal and the transverse directions, respectively. The design strength of concrete was 30 MPa. The reinforced concrete footing that supported P1 was 5.3m long and 14m wide in the longitudinal and the transverse directions, respectively. Eight one m-diameter cast-in-

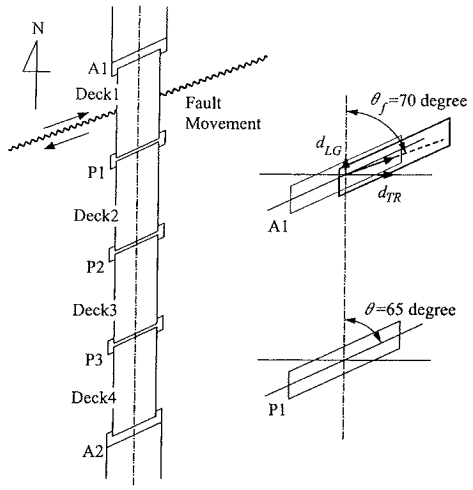

Fig. 5 Arfiye Bridge

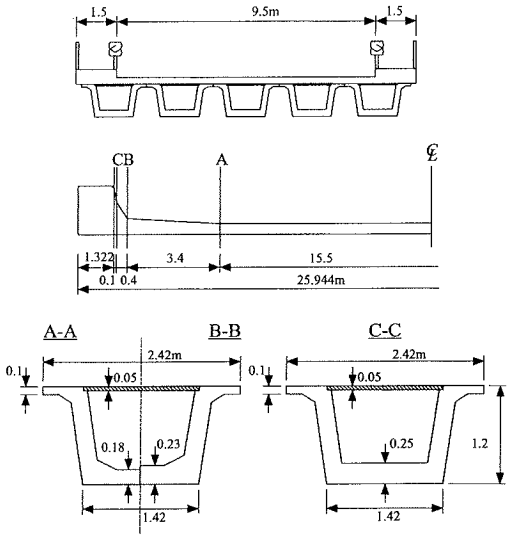

Fig. 6 Cross Section of Arifiye Bridge
(Courtesy of F.Inal and H. Hoashi)

place reinforced concrete piles supported the footing of P3.

The piles were reinforced by twelve 20mm plain bars. The averaged concrete strengths measured by the author using the Shumit hammer were 56 MPa and 47 MPa at the front wall of A2 and the upper surface of P1 footing, respectively. They were high enough for the normal reinforced concrete piers and abutments.

As shown in **Fig. 5**, the fault crossed the bridge between A1 and P1 at an angle θ of 70-degree. The right-lateral strike-slip fault dislocated A1 in northeast direction relative to P1-P3 and A2. If one idealizes the ground displacements as shown in **Fig. 8 (a)**, the ground displacements at north and south

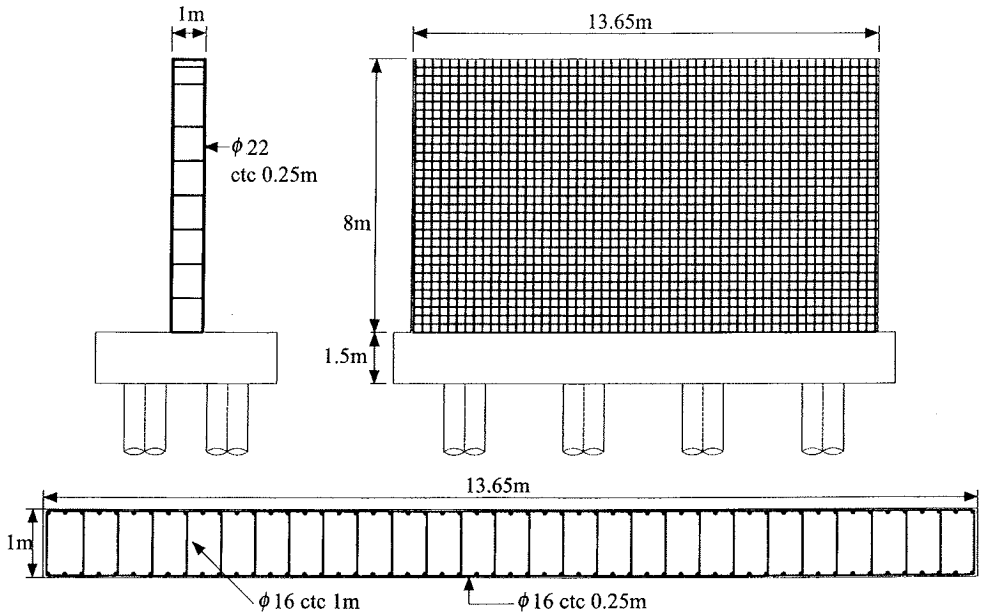

Fig.7 Section of Piers, Arifiye Overpass (Courtesy of F.Inal and H. Hoashi)

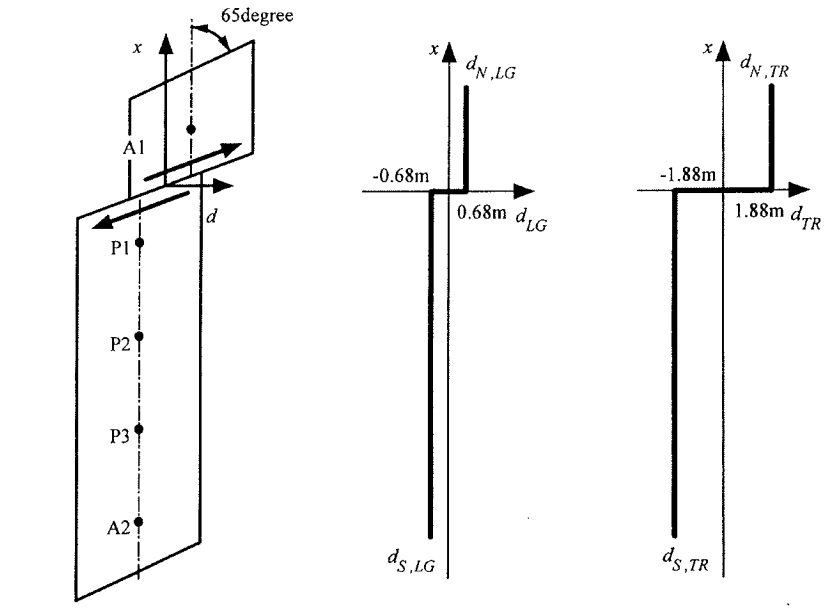

(a) Deformation of Ground (b) Displacement d_{LG} (c) Displacement d_{TR}

Fig.8 Effect of Fault Movement

tips, d_N and d_S, may be obtained as $d_N = d_S = D_0/2$, in which D_0 is the displacement of the fault dislocation. Hence, the ground movement in the transverse and the longitudinal directions of the bridge axis may be represented

$$d_{N,TR} = D_0/2 \cdot \sin\theta$$
$$d_{N,LG} = D_0/2 \cdot \cos\theta \quad (1)$$

at the north tip of the fault, and

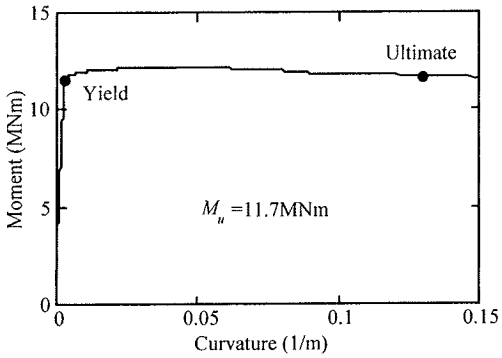

(a) Moment-Curvature Relation

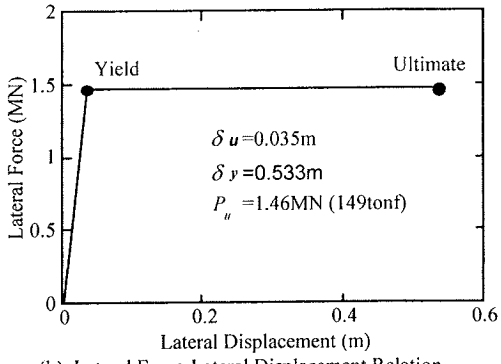

(b) Lateral Force-Lateral Displacement Relation

Fig.9 Lateral Force vs. Lateral Displacement of a Wall Pier, Arifiye Overpass

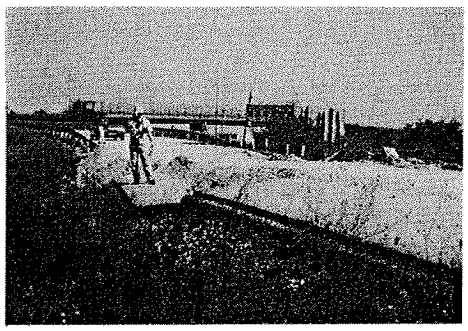

Photo 7 Minor Damage in an Overpass where the Fault Crossed the Overpass at the Abutment

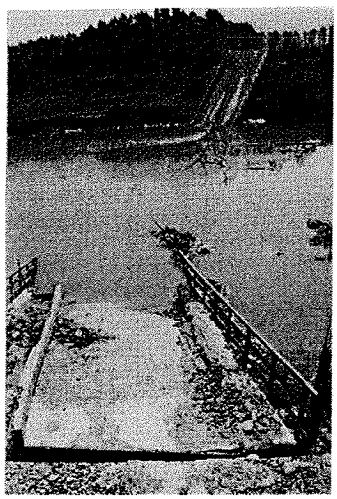

Photo 8 Collapse of Sakarya Central Bridge

$$d_{S,TR} = -D_0/2 \cdot \sin\theta$$
$$d_{S,LG} = -D_0/2 \cdot \cos\theta \qquad (2)$$

at the south tip of the fault.

Assuming $D_0 \approx$ 4m and $\theta \approx$ 70-degree, the ground displacements may be evaluated from Eqs. (1) and (2) as shown in **Fig. 8 (b)** and **(c)**. The

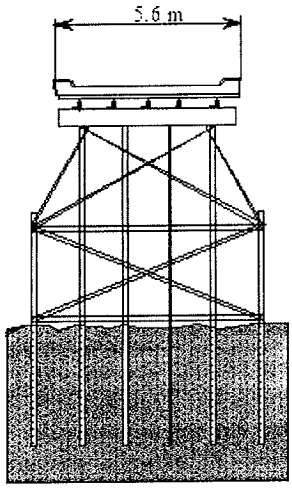

Fig.10 Sakarya Central Bridge (Courtesy of K. Kosa)

relative displacement between A1 and P1 in the longitudinal direction, d_{LG}, was 1.37m, which was much larger than the seat length of 0.6 m at A1 and 0.45 m at P1. It seemed that D1 dislodged from their supports resulting from such a large relative displacement between A1 and P1. On the other hand, the foundations of P2, P3 and A2 were dislocated in south direction. It appeared that such a southward movement of the foundations resulted in the dislodgments of D2, D3 and D4 from their supports at the north end.

Based on the reinforcement presented in **Fig. 7** and the concrete strength of 30 MPa, the lateral force vs. lateral displacement relation was evaluated based on the standard moment-curvature analysis[5] as shown in **Fig. 9**. The stress-strain relation of concrete by Hoshikuma et al[6] was used to represent the confinement effect. Assuming that the tributary

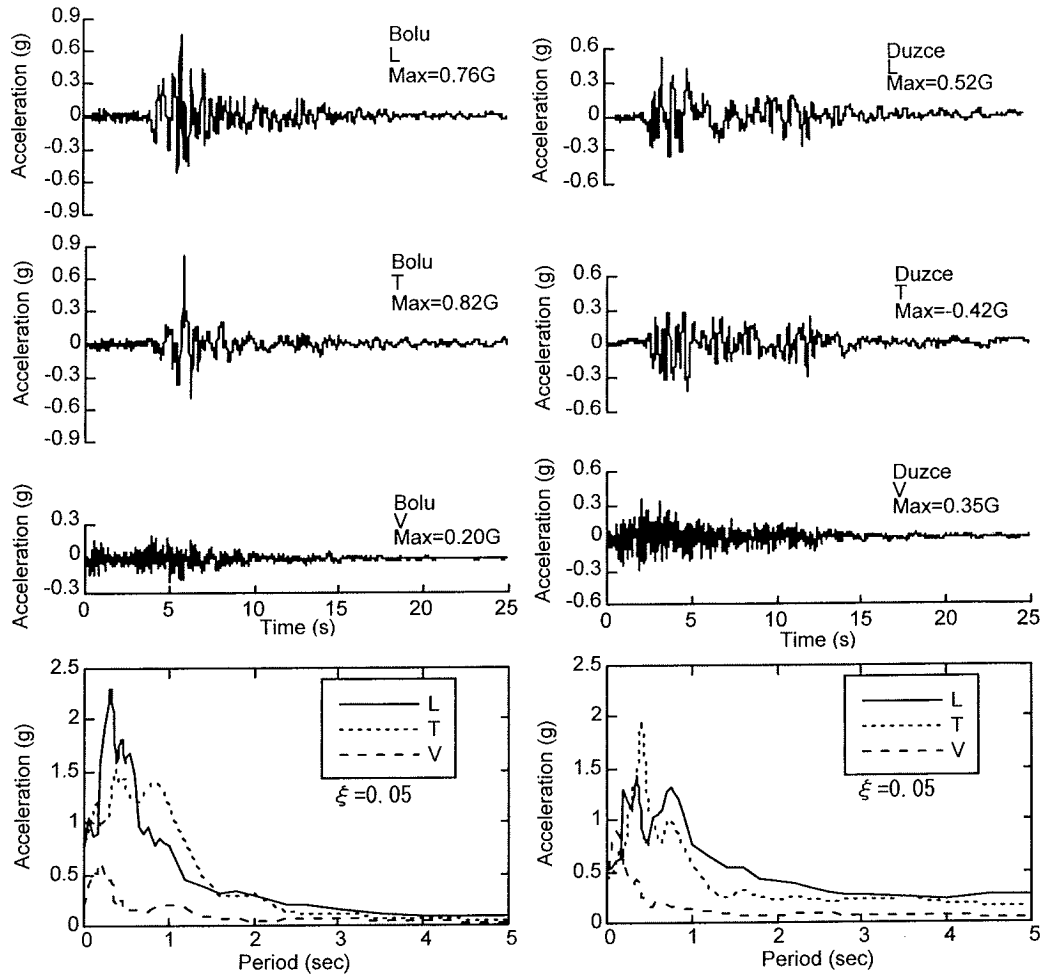

(a) Bolu (b) Duzce

Fig.11 Ground Accelerations in the Duzce Earthquake

mass of a pier was 5800 kN, the response acceleration that resulted in the yielding of a pier is approximately 0.3 g. This is the yielding level of bridge piers designed in accordance with the Japanese design codes using a 0.25 seismic coefficient.

(3) Overpasses around Arifiye Overpass

Near the Arifiye Overpass, there existed several overpasses that had the decks and the substructures similar to the Arifiye Overpass. In general, their seismic performance was satisfactory. For example, the fault crossed a two span simply supported prestressed concrete overpass (No. 1 Overpass, refer to **Fig. 3**) at its south abutment, after crossing the Motorway at about 50 m west of the overpass as shown in **Photo 7**. However, the damage was limited, i.e., only about 50mm-shear deformations of elastomeric bearings occurred resulting from the fault movement.

At a 3 span simply supported overpass (No. 2 Overpass, refer to **Fig. 3**), located about 400m east of No. 1 Overpass, the deck collided with the north abutment, resulting in a crush of a part of the concrete parapet walls. About 20-30mm-shear deformations of the elastomeric bearings occurred due to the fault movement. A 3 span simply supported overpass located about 400m west of the Arifiye Overpass (No. 4 Overpass, refer to **Fig. 3**) suffered only minor damage at the parapet walls of the north abutment, although the fault crossed near the south abutment.

The short wall piers, the short bridge spans and

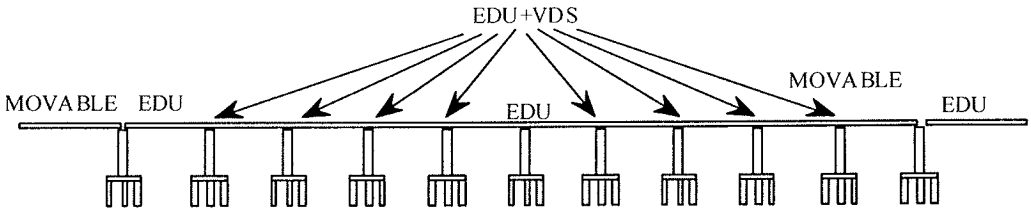

Fig.12 Supporting Condition of Typical 10-Span Continuous Deck (EDU: Energy Dissipating Unit, VDS: Viscous Damper Stopper, Movable: Sliding Pot Bearings)

the large restrain of the rigid abutments on the deck prevented the build-up of the bridge response in the earthquake.

(4) Sakarya Center Bridge

Sakarya Center Bridge, crossing Sakarya river, on a regional road (No. 5 bridge, refer to **Fig. 3**) collapsed as shown in **Photo 8**. The bridge consisted of eight span simply supported girders with two internal hinges (Gerber hinges) at the center. It was 92m long (10m+6x12m+10m). Steel bent piles as shown in Fig. 10 supported them. It was constructed 30-35 years ago. The fault crossed the north abutment.

3. DUZCE, TURKEY, EARTHQUAKE

(1) Duzce Earthquake

A part of the Istanbul-Ankara Motorway at Bolu (Bolu Viaduct) suffered extensive damage in the Duzce Earthquake[1), 3), 7)] (refer to **Fig. 1**). **Fig. 11** shows the ground accelerations recorded at Bolu and Duzce in the Duzce Earthquake[4)]. Bolu Viaduct was close to these stations. The peak accelerations of the two lateral components were 0.76 g and 0.82 g at Bolu. The long period pulses were included in the records. Response acceleration of 0.05 damping ratio was 2.3 g in the L-component.

(2) Bolu Viaduct

Bolu Viaduct consisted of a westbound bridge and an eastbound bridge as shown in **Photo 9**. There existed 59 spans and 58 spans in the westbound bridge and the eastbound bridge, respectively. Averaged span length was 40m. The total deck length was 2313m and 2273m in the west bound and the east bound bridges, respectively. The

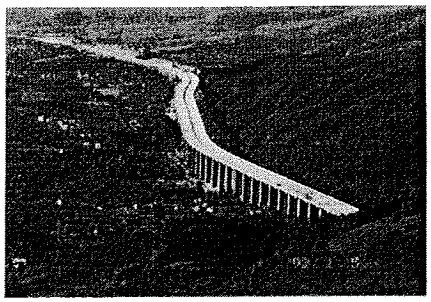

Photo 9 Bolu Viaduct

superstructure consisted of seven prestressed concrete U-beams placed in the transverse direction, and they were connected together by reinforced concrete decks. Although the U-beams were simply supported, the concrete decks were continuous over 10 spans. Hence, the Viaduct behaved as 10 span continuous bridges.

Reinforced concrete piers with heights from 10m to 49m supported them. Most piers were taller than 40m. Pile foundations supported the piers. A pile foundation consisted of 12 1.8m diameter piles and a 3m thick 18.7m wide and 16m long footing. Pile depths varied from 15m to 40m depending on the soil condition.

When the Duzce Earthquake occurred, the Viaduct was almost completed, i.e., the foundations, the piers, and the decks were completed, and only the pavement was not ready.

A unique supporting system was adopted in Bolu Viaduct1[4)]. As shown in **Fig. 12**, in a standard 10 span continuous bridge with a length of 10x40m=400m, the deck was supported by the pot bearings that allowed the decks to move multi-directionally. An energy-dissipating unit (EDU in **Fig. 12**) was provided at 10 piers, except one of the two deck ends. They achieved the energy dissipation for the multi-directional movements of the deck in an earthquake. Except at one of the two deck ends and the mid-pier, a viscous damper

stopper (VDS in **Fig. 12**) was provided. It was connected to the energy-dissipating unit in series.

The viscous damper stoppers allowed the free movements of the deck in the longitudinal direction due to the creep, the shrinkage and the thermal effects. Under the strong excitations, the viscous damper stoppers are locked, so that the energy dissipating units dissipated the energy. ALGA S.p.A mechanical hysteretic dampers consisting of 8 C-shaped mild steel damping elements were used as the energy dissipating unit.

At one of the deck ends, the energy-dissipating unit was provided to constrain the deck movement relative to the pier. At the other deck end, the deck could move freely in the longitudinal direction. In the transverse direction, the energy dissipating devices were provided at both deck ends. A set of cable restrainers was provided at the deck ends to prevent excessive relative displacement between the decks.

The site was located at the complex transition area between the Duzce fault and the North Anatoria fault. From the preliminary design stage, it was known that the site is seismically active and fault offsets were anticipated[3]. The Viaduct was designed assuming the peak ground acceleration of 0.4g in accordance with the 1983 AASHTO Specifications[8] with some modifications. The important modification from the AASHTO Guide Specifications was the response modification factor R; Although AASHTO specified a value of R=3 for single columns, R=1 was used in the design of Bolu Viaduct to ensure the elastic response in the piers[3].

(3) Damage of Bolu Viaduct

Prior to the Duzce Earthquake 9, Bolu Viaduct experienced the Kocaeli Earthquake. Although the epicenter of the Kocaeli Earthquake was about 100km away from the Viaduct, it was not far from the east bound of the tectonic fault zone. The energy dissipating units experienced the elastic movements in the range of 44-80mm[3] during this earthquake.

The epicenter of Duzce Earthquake was about 6 km south of Duzce, and Bolu Viaduct was close to Duzce. The fault crossed the Bolu Viaduct at Pier 45 and Pier 47 at an angle of approximately 20-30 degrees with the bridge axis. The right lateral offset

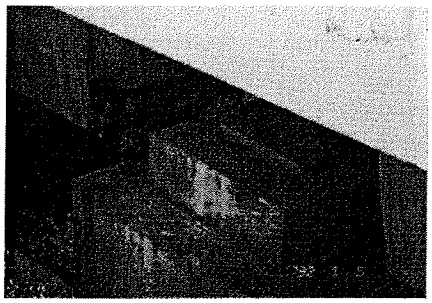

Photo 10 Girder Offset from the Pier

Photo 11 Shear Failure of Deck resulting from the Offset of Girder from the Pier

was approximately 2-2.5m[3].

Most decks moved in the longitudinal and the transversal directions. At several piers, the girders offset from their pedestals, and were hung only by the concrete slabs as shown in **Photo 10**. Consequently, the concrete slabs suffered extensive shear failure as shown in **Photo 11**. Some decks were about to collapse. Based on the site inspection, it seemed that the most decks in the west from the fault rupture moved in the west direction while the most decks in the east of the fault moved in the east direction. If this is correct, the direction of the movements of the decks was not consistent to the right lateral slip. This requires more detailed survey of the damage.

Photo 12 shows a damage of the energy-dissipating unit and the viscous damper stopper at Pier 48R. The C-shaped energy dissipating elements suffered damage, as shown in **Photo 13**, due to an excessive movement of the deck. 30mm diameter bolts that connected the elements to the frame ruptured. **Photo 14** shows a set of cable restrainers at a deck end. It seemed that the cable restrainers were effective to prevent collapse of the Viaduct

Some pile foundations where the fault crossed the Viaduct rotated[9]. **Photo 15** shows the damage investigation of piles by removing the soils.

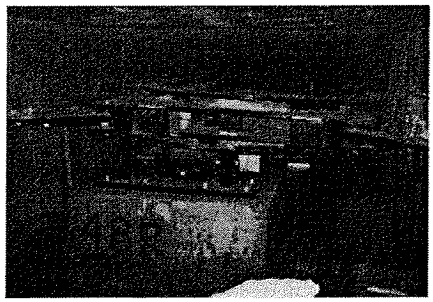

Photo 12 Damaged Energy Dissipating Unit and Viscous Damper Stopper

Photo 13 Energy Dissipating Elements that suffered Damage resulting from Excessive Movement of the Deck

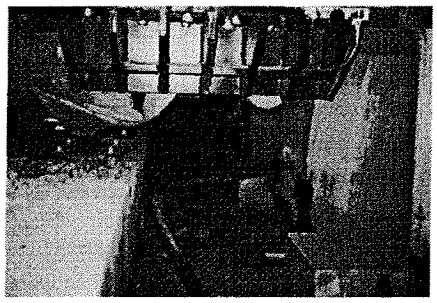

Photo 14 Cable Restrainers

4. CHI-CHI, TAIWAN EARTHQUAKE

(1) Fault displacements and ground motions

The Che-Long-Pu Fault induced the earthquake. It was a thrust fault, and surface ruptures occurred over 70km between Min-Ju and Tungshih. Eastern Taiwan is a tongue of the Philippine Sea tectonic plate that is over-thrusting the Eurasia plate. As shown in **Fig. 13**, damage occurred in Shihkang region, Tungshih region, Taiping, Wufeng and

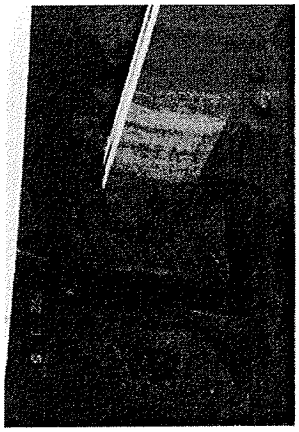

Photo 15 Damage Evaluation of Pile Foundation

Tsaotun region, Nantou region, Chi Chi region, and Mingchien and Chushan region.

Figs. 14 and **15** show the ground accelerations recorded at Shikhkang (TCU068), Taichung (TCU082) and Nantou (TCU076) and their response acceleration of 0.05 damping ratio, respectively[10]. Longer period pulses were included in the ground accelerations measured at the north. In particular, the EW component at Shikhkang had a single pulse with the peak acceleration of 4.9 m/s^2. The response acceleration of 0.05 damping ratio was about 1.5g at 0.5 second in the record.

Fig. 16 compares the record at Shikhkang (TCU068) with the records at Bolu (L-component) and Duzce (L-component) in the Duzce Earthquake (refer to **Fig. 11**), Sylmar parking lot (NS-component) in the 1994 Northridge Earthquake and JMA Kobe Observatory in the 1995 Hyogo-ken Nanbu Earthquake. It is noteworthy that the JMA Kobe record had the highest response accelerations at 0.5-1 second, while the Shikhkang record had the highest response accelerations at natural periods over 2 second.

In the Chi Chi Earthquake, at least eight bridges (Bei-Fong Bridge, Chang-Geng Great Bridge, Shc-Wci Bridge, Yi-Jian Bridge, Wu-Shi Bridge, Pin-Ling Bridge, Mou-Loh-Shi Bridge, Min-Ju Great Bridge, and Tong-Tou Bridge) collapsed, and a number of bridges suffered extensive damage[1), 11), 12), 13)]. Most of the extensive damage resulted from the fault displacement effects. Two bridges that suffered damage from the fault movement are described below.

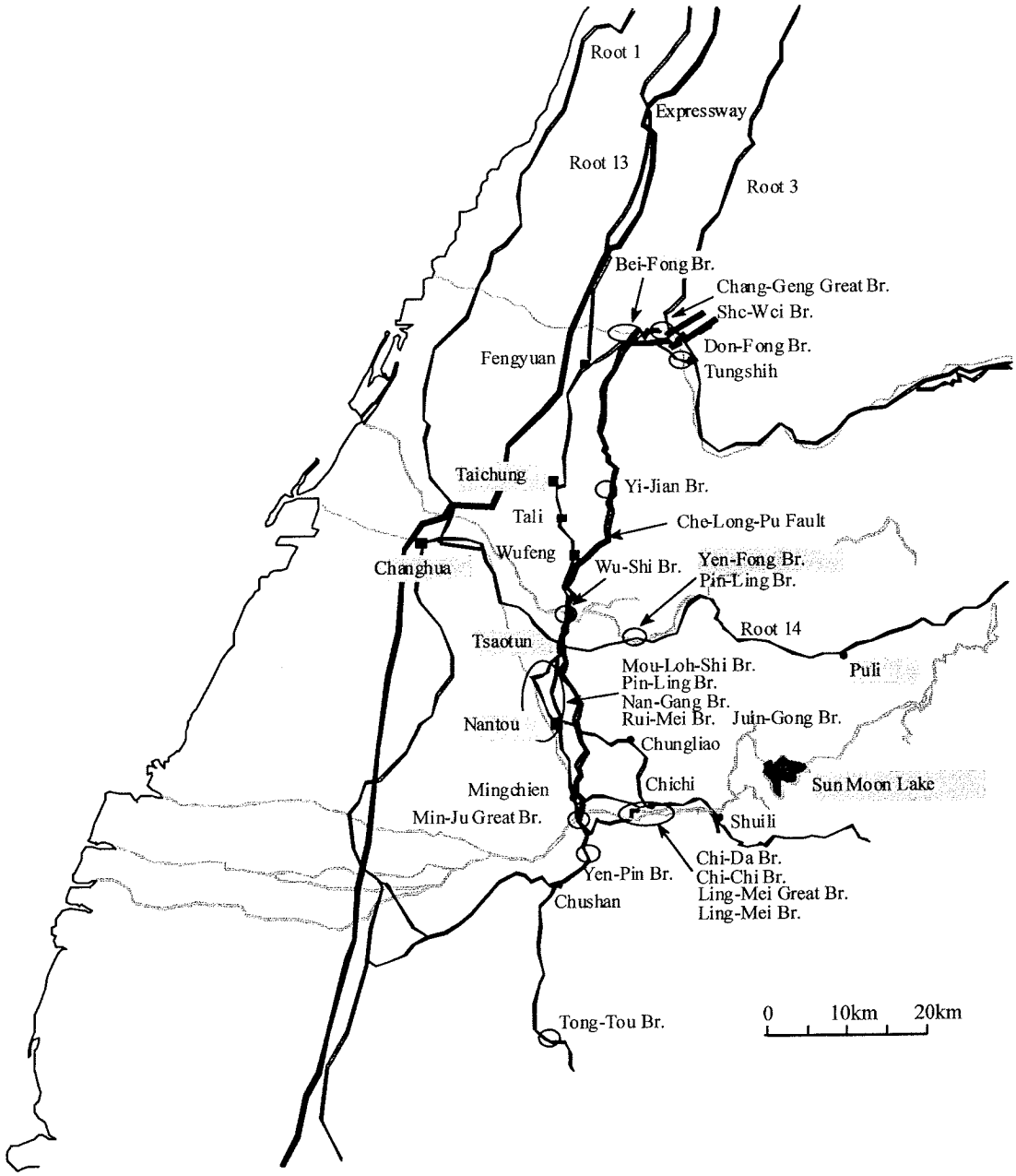

Fig.13 Damaged Bridges, Chi-Chi Earthquake

(2) Collapse of Bei-Fong Bridge

Bei-Fong Bridge was located downstream of the Shikhkang Dam. Resulting from the fault rupture, a waterfall was created about 100m upstream of the bridge. It was a 13-span simply supported I-beam girder bridge constructed in 1991. The south most three spans collapsed as shown in **Fig. 17** with other spans being free from damage. The abutments, the piers and the decks are numbered herein from the north to the south. A2, P12 and P11 up-heaved about 3-4m, and P12 and A2 were laterally displaced about 3.5m and 4m, respectively, in the downstream direction (west) as shown in **Photo 16**. D13 was resting on the slope of the river embankment with the north end being dislodged 6.6m south from the original alignment.

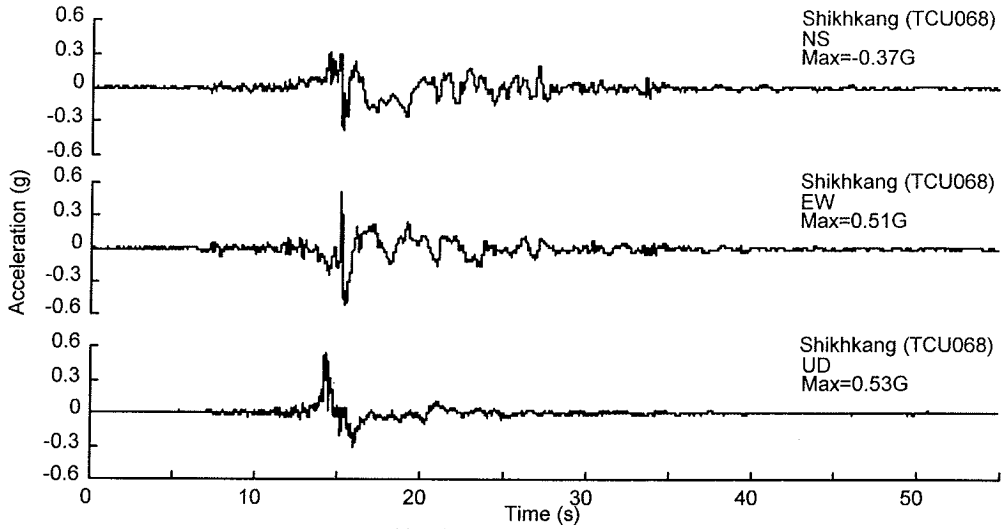

(a) Shikhkang (TCU068)

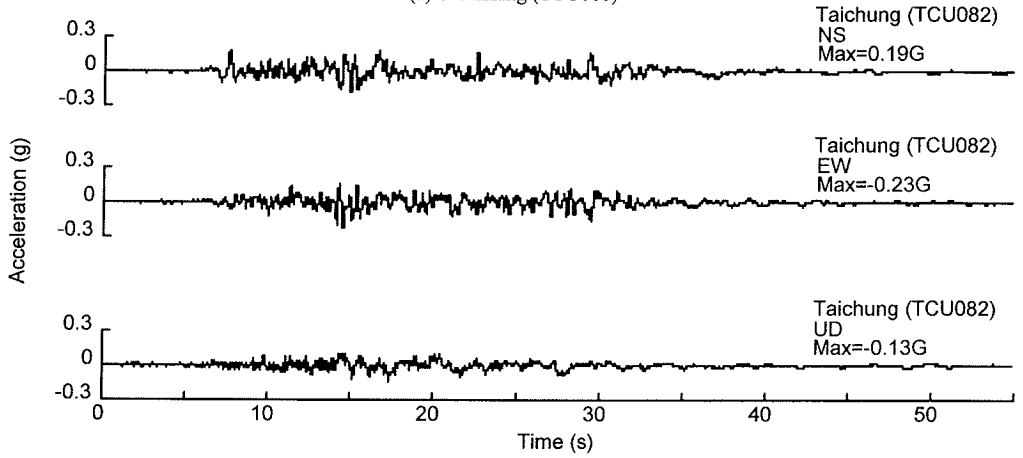

(b) Taichung (TCU082)

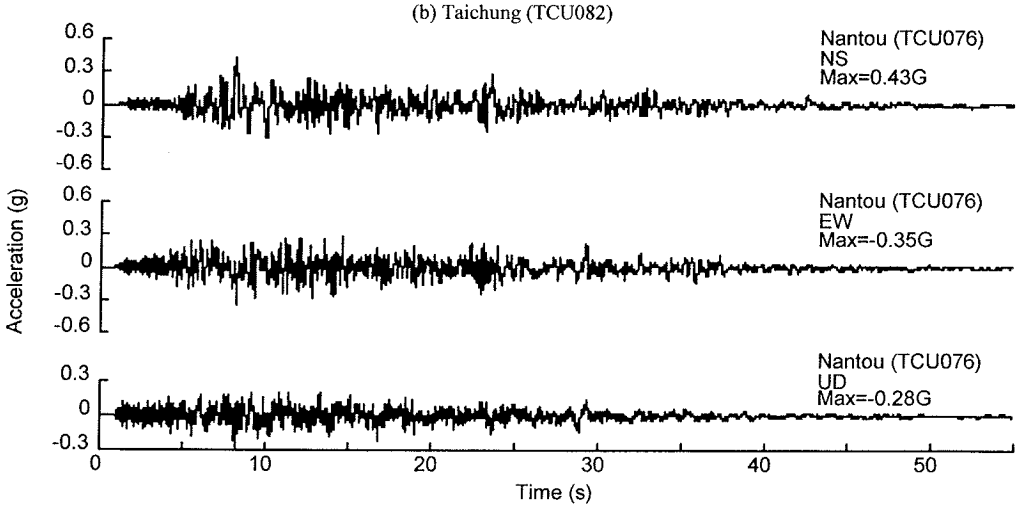

(c) Nantou (TCU076)

Fig.14 Ground Accelerations, Chi-Chi Earthquake

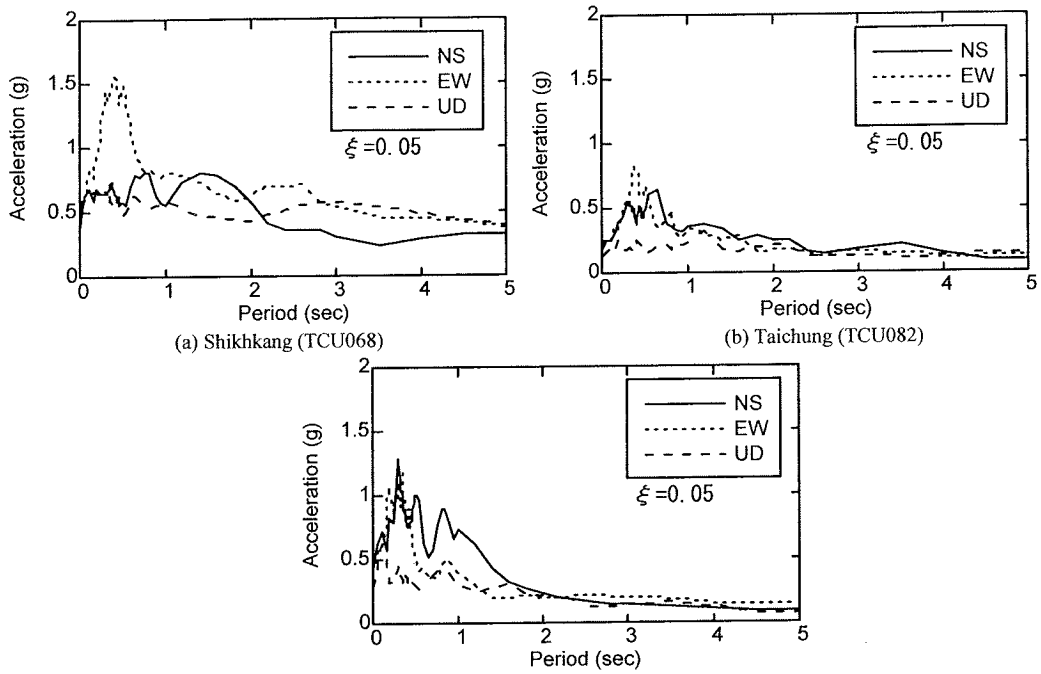

(a) Shikhkang (TCU068)

(b) Taichung (TCU082)

(c) Nantou (TCU076)

Fig.15 Response Acceleration with 0.05 Damping Ratio, Chi-Chi Earthquake

Fig. 18 shows the location of fault investigated by the Taiwan Geological Survey and Otsuki, K., Tohoku University. It seems that the fault crossed the bridge between A2 and P12 at an angle of about 42-degree. From the fact that P12 was laterally displaced in west, and that D11 and D12 clock wisely rotated (20-40-degree), it appeared that the fault rupture crossed the bridge between A2 and P11 as shown in **Fig. 19**.

If one idealizes the fault rupture at the south tip of the fault relative to the north tip, the transverse and the longitudinal displacements of the ground may be represented as (refer to **Fig. 19**)

$$\begin{aligned} d_{TR} &= -D_0 \sin\theta \\ d_{LG} &= -D_0 \cos\theta \end{aligned} \tag{3}$$

in which D_0 is the fault displacement. Substituting $d_{TR} \approx$ -4m and $\theta \approx$ 42-degree into Eq. (3), one obtains $D_0 \approx$-6m and $d_{LG} \approx$-4.5m. Although the longitudinal displacement $d_{LG} \approx$-4.5m is not large enough to the above-estimated southward dislodgment of D13 at the north end (6.6m), they are not too much different.

It is interesting to note that the vertical upheaval might not be a serious cause of the dislodgment of the decks from their supports. If one idealizes the upheaval of the right substructure relative to the left as shown in **Fig. 20**, the shortening of span length resulting from the upheaval, Δl, may be written as

$$\Delta l = \frac{1}{\cos\theta_V}(1 - \cos\theta_V) \tag{4}$$

in which θ_V is the angle of tilting, and is given as

$$\theta_V = \tan^{-1}(d_V / l) \tag{5}$$

in which l is the span length and d_V is the amplitude of relative upheaval between two substructures. Assuming $\Delta l \approx$ 25m and $d_V \approx$ 3m, one obtains θ_V =6.8 degree and Δl =0.18m. Consequently, the shortening of the span length resulted from the upheaval is much shorter than the seat length.

Based on the above facts, it seems that the collapse of the bridge resulted from a large tilting of P11 in the north direction, which was caused by the fault movement as shown in **Fig. 21**. D12 dislodged

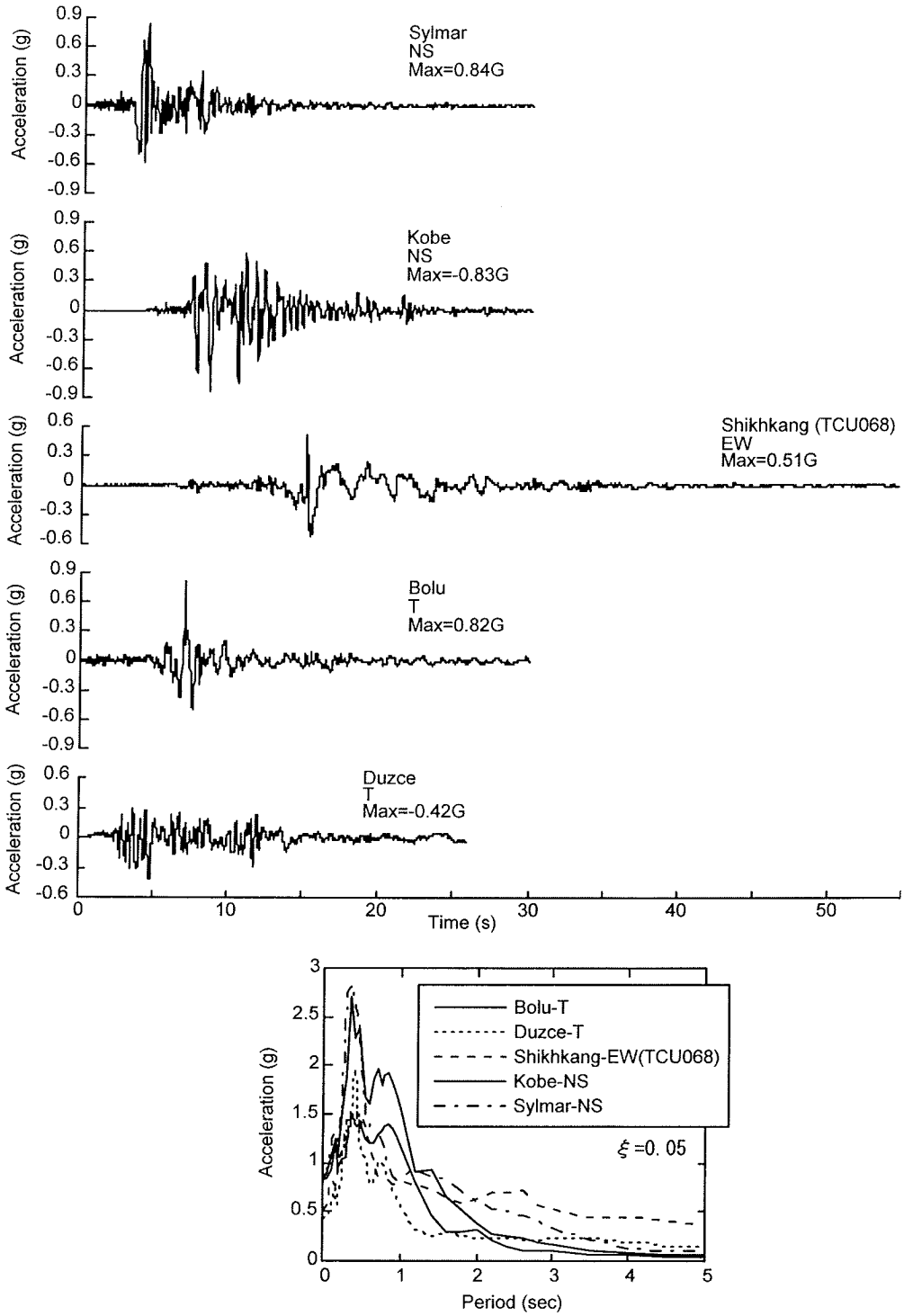

Fig.16 Comparison of Strong Motion Accelerations in the Duzce, Chi-Chi, Northridge, and Hyogo-ken Nanbu Earthquakes

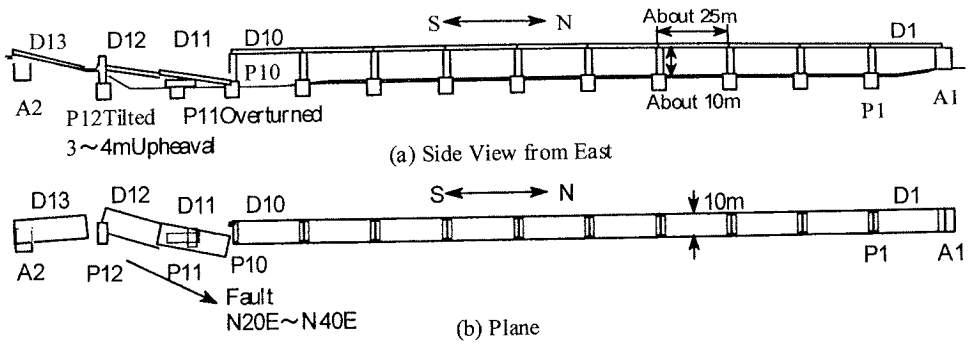

Fig.17 Damage of Bei-Fong Bridge

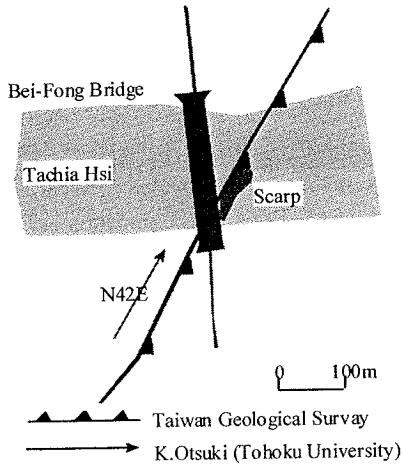

Fig.18 Fault around Bei-Fong Bridge

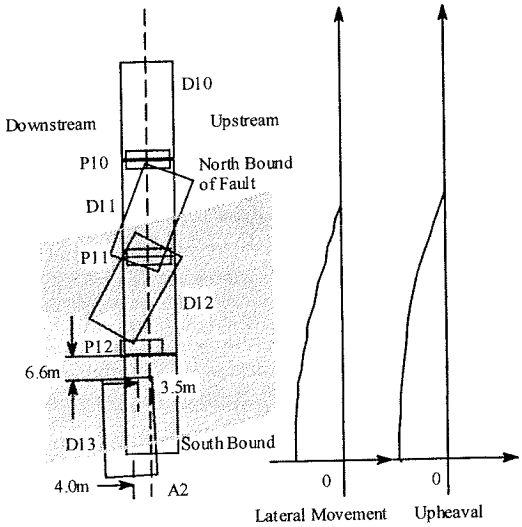

Fig.19 Fault Movement and Ground Movement, Bei-Fong Bridge

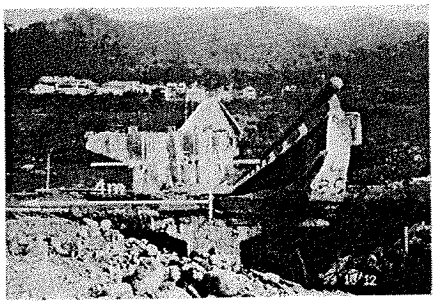

Photo 16 Lateral Movement of A2 and P2, Bei-Fong Bridge

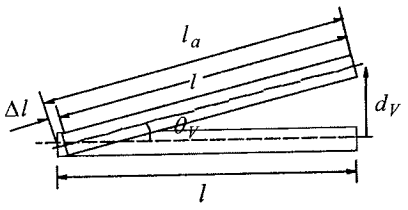

Fig.20 Shortening of Span Length due to Upheaval

from P11 first at its north end, followed by the dislodgment at the south end. This resulted in the complete collapse of D12. D12 finally felt on P11 at the north end with the clockwise rotation resulting from the right-lateral fault. The collapse of P11 resulted in the dislodgment of D11 at its south end. The south end of D11 thus finally collapsed on the north end of D12. Increased distance between P12 and A2 resulted in the collapse of D13.

(3) Collapse of Wu-Shi Bridge

Wu-Shi Bridge consisted of a northbound bridge (upstream, east) and a southbound bridge (downstream, west) as shown in **Fig. 22**. Each bridge consisted of 17-span simply supported PC beam girders. Bridge axis was N20E. The

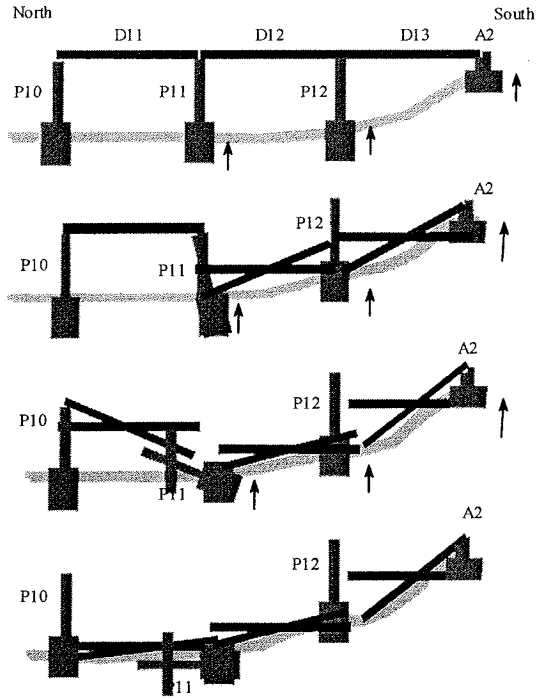

Fig.21 Collapse Mechanism, Bei-Fong Bridge

abutments, the piers and the decks are numbered herein from the north to the south, and the northbound and the southbound bridges are identified by putting the subscripts "E" and "W," respectively.

The northbound bridge was constructed in 1983, while the southbound bridge was newer than the northbound bridge. As shown in **Photo 17**, the northbound bridge was supported by 8.5m wide and 3m long wall piers, while the southbound bridge was supported by 5m wide and 2m long rectangular reinforced concrete piers. For example, in P1W (P1 at the southbound bridge), 32 deformed 22mm diameter bars were placed around the pier, and deformed 12mm diameter tie bars were placed at 200mm interval. They were supported by caisson foundations with a diameter of 6m. Deformed 22mm bars from the caissons were spliced with the bars from the piers at 1m above the bottom of piers. The concrete strength measured by the author using the Shumit hammer was about 24MPa.

D1E and D2E collapsed (refer to **Fig. 22**), while D1W and D2W tilted and settled extensively. **Fig. 23** shows the damage of piers in the southbound bridge. P1W and P2W failed in shear from the east to the west. The caisson foundation at P3W suffered shear failure from the east to the west as shown in **Photo 18**. Nearly all piers in the westbound bridge suffered damage. In particular, P1W and P2W suffered extensive damage.

On the other hand, the damage of P2E and P3E was limited; P2E suffered several shear cracks from the

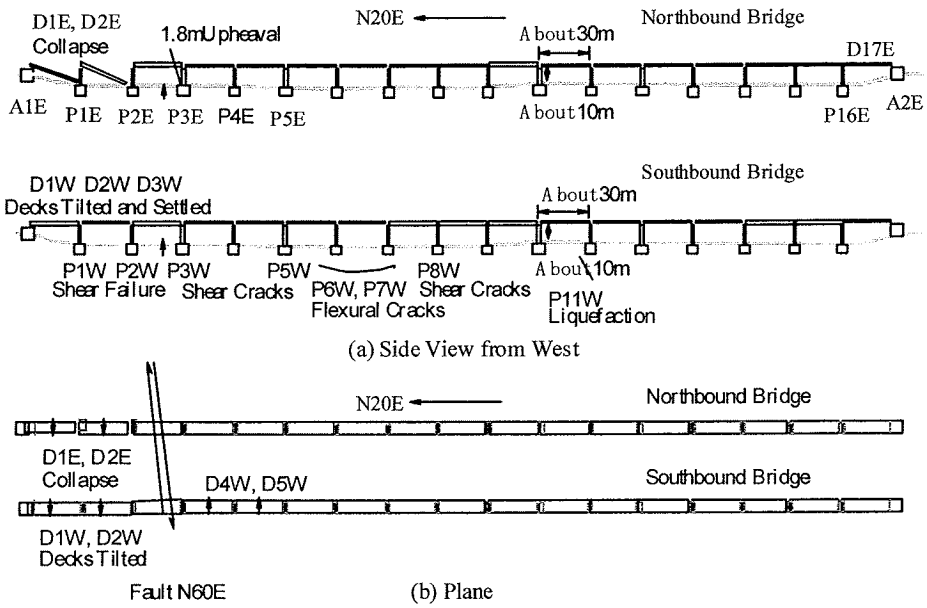

Fig.22 Damage of Wu-Shi Bridge

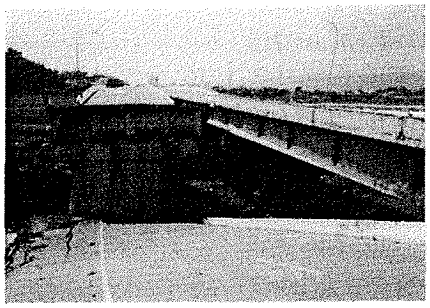

Photo 17 Collapse of Wu-Shi Bridge

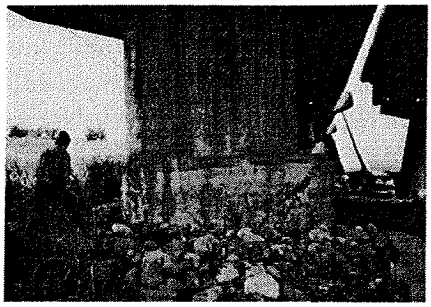

Photo 18 Shear Failure of Caisson Foundation Resulting from Fault Movement, Wu-Shi Bridge

north to the south at mid-height. P3E suffered a 100-150mm opening of concrete at 1.5m high from the foundation. It seems that P2E and P3E settled about 2m relative to the piers beyond P4E in the south. It seems that this was resulted from the upheaval in the south tip of the fault relative to the north tip.

A 2m high scarp was observed at about 100 m east (upstream) of the bridge. The fault crossed the bridge between P2 (P2E & P2W) and P3 (P3E & P3W) at an angle of about 40-degree (N60E) as shown in **Fig. 24**. **Photo 19** shows the eastward (transverse direction) displacement of P1W relative to other piers in the south of P3. The displacement was as large as 2m. However based on **Fig. 24**, it seems that the ground at the south tip of the fault moved in the west direction, and that this resulted in the shear failure from the east to the west in P1W and P2W.

Substituting the relative displacement in the transverse direction of $d_{TR} \approx 2$m and $\theta \approx 40$-degree into Eq. (3), the fault displacement is estimated as $D_0 \approx 3.1$m, and the relative displacement in the longitudinal direction d_{LG} is estimated as about 2.4m. It seems that the westward fault movement at the south of P3W resulted in a lateral force to occur in D1W and

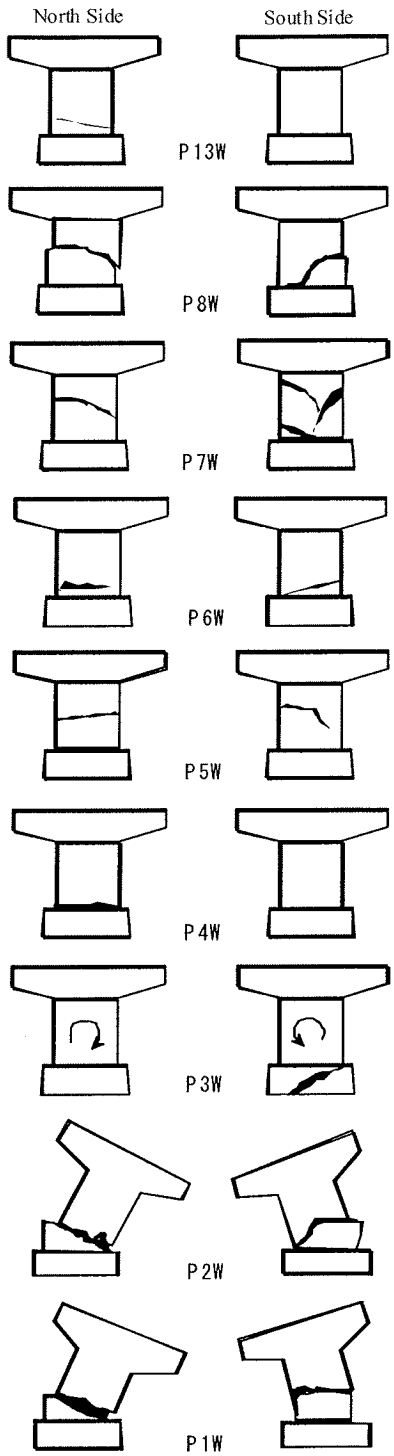

Fig.23 Failure of Piers, Wu-Shi Bridge

D2W in the west direction, which, in turn, caused the shear failure in P1W and P2W. It seems that since the failure of P1W and P2W contributed to absorb the large fault displacement, the decks

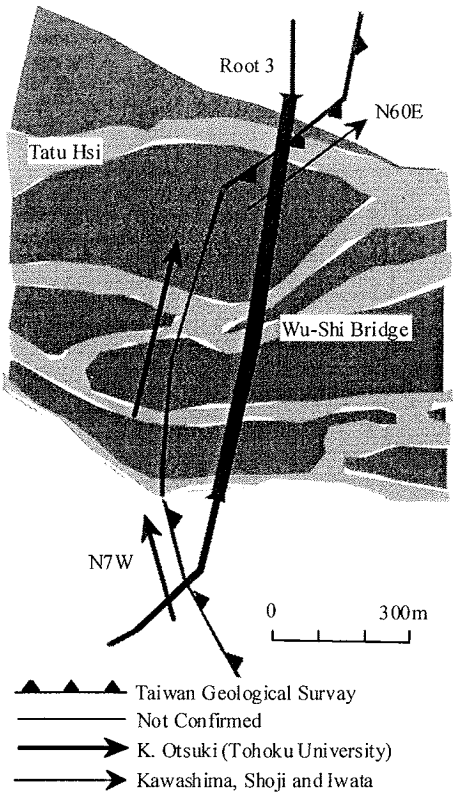

Fig.24 Fault around Wu-Shi Bridge

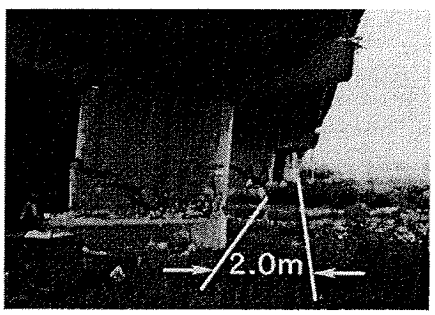

Photo 19 Lateral Movement of P1 and P2, Wu-Shi Bridge

(D1W and D2W) did not collapse.

In a similar way, D1E and D2E in the northbound bridge were subjected to a large lateral force, which resulted in limited damage at P1E and P2E. Since the strength of wall piers (P1E and P2E) was large, they did not collapse. Therefore, the large relative displacements between the piers and the decks occurred, which resulted in the collapse of D1E and D2E.

It seems that the failure of the caisson foundation at P3W (refer to **Photo 18**) resulted from the fault movement.

5. CONCLUSIONS

Seismic damage of bridges resulting from the fault ruptures in the 1999 Kocaeli and Duzce, Turkey, Earthquakes, and the 1999 Chi-Chi, Taiwan, Earthquake was presented. Features of the damage may be summarized as follows:

(1) The fault ground movements that crossed the bridges resulted in the extensive damage in Kocaeli, Duzce and Chi-Chi Earthquakes.

(2) In Kocaeli Earthquake, Arifiye Overpass collapsed resulting from a fault rupture that crossed the bridge at an angle of 65-degree. An increased distance between A1 and P1 resulted in the collapse of D1, and the lateral displacement of the foundations resulting from the fault rupture contributed to the damage of D2, D3 and D4. Because other overpasses on the Trans-Europe Motorway were rested on short and rigid wall piers and abutments, damage resulting from the fault rupture was less significant.

(3) In the Duzce Earthquake, Bolu Viaduct consisted of a 2.2km long bridge and a 2.3km long bridge suffered extensive damage resulting from the fault rupture that crossed the Viaduct. Since the deck movement was so large that the girders were offset from their supports. As a consequence, the Viaduct was about to collapse, but the reinforced concrete slabs prevented the collapse.

(4) In the Chi-Chi Earthquake, at least eight bridges collapsed. Bei-Fong Bridge and Wu-Shi Bridge suffered significant damage resulting from the fault rupture. The fault crossed the bridges, and this resulted in a large lateral force in the piers. The overturning and the failures of the piers resulted in the collapse of the bridges.

(5) It is interesting to note in Wu-Shi Bridge that the decks supported by the stiff reinforced concrete wall piers collapsed in the northbound bridge while the decks supported by the reinforced concrete piers with smaller rectangular sections did not fall down (although they suffered major damage) in the southbound bridge. The failure of the piers in the southbound bridge absorbed the fault displacements. It showed that a certain type of devices or mechanisms that absorb the fault

displacements is effective to prevent the failure of a bridge when it is subjected to a large fault movement.

ACKNOWLEDGEMENT: The author expresses his sincere appreciation to many organizations and individuals those kindly supported and provided the opportunities to survey the damage. In particular, the author thanks Mr. Yigit, D., KGM Director General, Ms. Inal F. and Tiras, A., KGM, Mr. Hoashi, H., Japanese specialist dispatched to KGM, and Professor Yilmaz, C, Middle East University, Turkey for their kind cooperation. The author thanks Drs. Philip Yen and Hamid Ghasemi, US Federal Highway Administration for providing an opportunity to visit the Bolu Viaduct in December 2000. The authors also sincerely appreciate Professors C. H. Loh and K. C. Chang, National Center for Research on Earthquake Engineering, National Taiwan University, Taiwan for their kind support for the site damage investigation. The cooperation of Mr. Hashimoto, T., Chiyoda Consultants, and Dr. Suzuki, T., Okumura Construction, for the site investigation in the Kocaeli Earthquake, and Mr. G. Shoji, Tokyo Institute of Technology, Professor Iemura, H., Kyoto University and Mr. Iwata, S., JR Tokai Consultants, for the site investigation in the Chi-Chi Earthquake is greatly appreciated. Valuable information for the damage in the Kocaeli and the Chi-Chi Earthquakes was provided by Professor Kosa, K., Kyushu Institute of Technology.

REFERENCES

1) Kawashima, K. and Shoji, G.: Damage of Transportation Facilities in the 1999 Kocaeli and Duzce, Turkey Earthquake and the 1999 Chi Chi, Taiwan Earthquake, 32 Joint Meeting, Panel on Wind and Seismic Effects, UJNR, NIST, Gaithersburg, MD, USA, 2000

2) USGS: Implications for Earthquake Risk Reduction in the United States from the Kocaeli, Turkey, Earthquake of August 17, 1999, Geological Survey Circular, 1999

3) Yilmaz, C.: Design Philosophy and Criteria for Viaduct No. 1, KGM and FHWA Workshop, KGM, Ankara, Turkey, 2000

4) Bogazici University Kandilli Observatory and Earthquake Engineering, Home Page, 1999

5) Japan Road Association: Part V Seismic Design, Design Specifications of Highway Bridges (in Japanese), Maruzen, Tokyo, 1996.

6) Hoshikuma, J., Kawashima, K., Nagaya, K. and Taylor, A., Stress-Strain Model for Confined Reinforced Concrete in Bridge Piers. *Journal of Structural Engineering*, vol.123, No.5, pp. 624-633, ASCE, New York, 1994.

7) Ghasemi, H., Yen, P. and Cooper, J. D.: The 1999 Turkish Earthquake: Post Earthquake Investigation of Structures on the Trans European Motorway, Proc. 2nd International Workshop on Mitigation of Seismic Effects on Transportation Structures, pp. 337-348, National Center for Research on Earthquake Engineering, Taipei, Taiwan, 2000

8) AASHTO: Guide Specifications for Seismic Design of Highway Bridges, 1983

9) Tiras, A. and Sahiss, T.: European Transit Motorway Damaged Bridge Restoration after Kocaeli and Bolu Earthquakes, 80th Annual Meeting, Transportation Research Board, Washington, D.C., USA, 2001

10) Lee, W. et al: CWB Free-field Strong Motion Data from the 921 Chi-Chi Earthquake, Vol. 1, Digital Acceleration Files on CD-ROM, 1999

11) Chang, K. C., Chang, D. W., Tsai, M. H. and Sung, Y. C.: Seismic Performance of Highway Bridges, *Earthquake Engineering and Engineering Seismology*, 2(1), pp. 55-77, 2000

12) Kosa, K., Adachi, Y., and Hsu, Y. T.: Evaluation of Earthquake Damaged Reinforced Concrete Piers by the Ultimate Bearing Capacity Procedure, Proc. 2nd International Workshop on Mitigation of Seismic Effects on Transportation Structures, pp. 173-186, National Center for Research on Earthquake Engineering, Taipei, Taiwan, 2000

13) Unjoh, S. and Kondoh, M.: Analytical Study on the Effect of Fault Displacement on the Seismic Performance of Bridge Structures, Proc. 2nd International Workshop on Mitigation of Seismic Effects on Transportation Structures, pp. 222-233, National Center for Research on Earthquake Engineering, Taipei, Taiwan, 2000

(Received August 20, 2001)